

Beryl stability in local hydrothermal and chemical environments in a mineralized granite

GREGOR MARKL AND JOHN C. SCHUMACHER

Institut für Mineralogie, Petrologie und Geochemie, Albert-Ludwigs-Universität, Albertstrasse 23b, D-79104 Freiburg i. Br., Germany

ABSTRACT

The temperature and chemistry of hydrothermal fluids control the breakdown and formation of beryl in rocks of appropriate bulk composition. In rocks of the Triberg granitic complex in the Schwarzwald, Germany, late-magmatic to hydrothermal greisen fluids interacted with beryl-bearing pegmatites and the leucogranitic host rocks over a range of temperatures, but the greisen overprint was not pervasive. As a result, it is possible to examine the effects of the greisen fluids on beryl stability and the host granitic rock over a range of temperatures. Replacement of primary (pegmatitic) beryl resulted in the formation of secondary beryllium minerals. At high temperature (~550 °C), gem-quality aquamarine was precipitated in vugs with alteration halos of albite, muscovite, cassiterite, and fluorite. At lower temperatures (~250 °C), blue anhedral beryl replaced potassium feldspar in granite adjacent to fractures. At slightly lower temperatures (~220–230 °C), pegmatitic beryl was replaced by kaolinite ± bertrandite ± phenakite.

Calculated activity and phase diagrams suggest that precipitation of secondary beryl depends chiefly on variations in the ratio Na/K in the fluid. These same fluids were responsible for the albite and white mica formation in the surrounding granite. Further, the effective fluid-to-rock ratio determines the progress of the alteration reactions, which in turn determines the ability of the fluid to precipitate beryl. On the basis of fluid-inclusion measurements and the activity-diagram calculations, a pH of about 5 (at ~550 °C and 4% NaCl equivalent) was estimated for the fluids that caused the mineralization.

INTRODUCTION AND GEOLOGIC SETTING

The Triberg granite complex (Fig. 1) in the central Schwarzwald, southwestern Germany, is a composite Variscan batholith that is composed of granodiorite, monzogranite, leucogranite, and a transitional leucogranite, which is believed to represent a hybrid of the monzo- and the leucogranitic melts (Schleicher 1978, 1984, 1994; Schleicher and Fritsche 1978). Werchau et al. (1989) determined an intrusion age of 325 ± 5 Ma (U/Pb in monazite).

The leucogranite is the youngest of these granitic bodies and crosscuts the other units. The leucogranitic melt was water undersaturated and interpreted as the product of a low degree of partial melting of metamorphosed sedimentary rocks in the lower crust during the relaxation after the collisional stage of the Variscan orogeny (Schleicher 1994). The leucogranite consists of potassium feldspar, quartz, plagioclase (An_{0-22}), muscovite, biotite [$Fe/(Fe + Mg) = 0.93-0.95$], and pinite pseudomorphs after cordierite (Schleicher 1994). The SiO_2 content ranges from 76 to 79%, the Al_2O_3 content from 12 to 13.7%, and the total volume of mafic minerals is <5%. Contents of REE, Zr, Ba, and Sr are low, and Th, Y, Ga, and Rb/Sr are high (Schleicher 1994), which is typical for leucogranites. Additionally, the leucogranite contains small

pegmatitic lenses with tourmaline and, less commonly, beryl as well as cassiterite + fluorite + topaz greisen assemblages (Markl 1994; Markl and Schumacher 1996). However, the beryl and the greisen assemblages are concentrated in a small area of the leucogranite.

The greisen zone was described in more detail by Markl (1994) and Markl and Schumacher (1996), and only the main features are outlined below. The beryl- and cassiterite-bearing areas are nearly identical and restricted to a 4×8 km region that is centered around the village of Niederwasser (Fig. 2). In this area Markl and Schumacher (1996) showed that temperature and geochemical gradients in the fluids extended roughly radially outward from a center of greisen activity. Temperatures near the center of greisen activity were estimated to be about 550 °C at 1500 bar; at the margins of the greisen zone, fluid temperatures were about 250 °C at 1500 bar. The temperature decrease correlates with a decrease by a factor between 15 and 40 in a_{HF} of the fluids. The simplest model of these features is concentric gradients in temperature and composition of the greisen fluids. Accordingly, distance from the center of mineralization (Fig. 2) should give a rough estimate of the properties of the fluids. The formation of the primary beryl-bearing assemblages (pegmatites) was the earlier event, and the overprinting of it

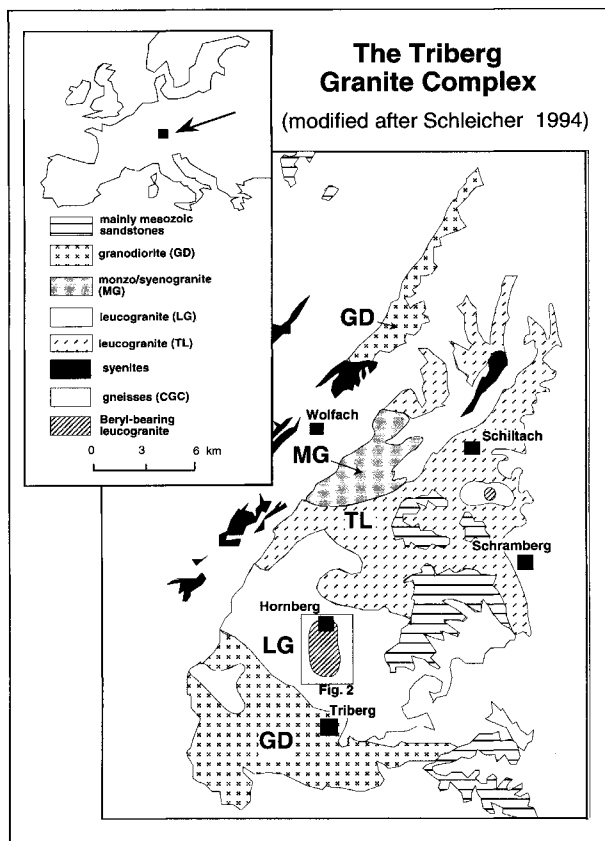


FIGURE 1. Generalized geologic map of the Triberg granite complex, modified after Schleicher (1994). Note the beryl-bearing areas in the leucogranite.

and partial remobilization of Be by the greisen fluids followed. On the basis of our observations the greisen emplacement was a short-lived single event.

Pegmatitic beryl occurrences, where Be^{2+} may be concentrated in late-magmatic, highly differentiated melts or fluids, are common worldwide and are major sources for gem-quality beryl (e.g., aquamarine). The breakdown of primary pegmatitic beryl by reaction with acid melt and the subsequent formation of chrysoberyl in pegmatitic environments was discussed by Franz and Morteani (1984). Late-magmatic and hydrothermal fluids play a major role in transporting Be^{2+} from the primary sources (e.g., pegmatites) to the locations where secondary beryllium minerals form (see Jahns and Burnham 1969). For example, Černý (1968) described more than 40 types of beryllium mineral associations that formed from the alteration of beryl. Burt (1975) discussed qualitatively the beryl breakdown in terms of $\mu_{\text{F}_2\text{O}_{-1}}$ and $\mu_{\text{P}_2\text{O}_5}$. Mårtensson (1960) and Tennyson (1960) described mobilization of primary pegmatitic beryl and formation of secondary Be minerals from hydrothermal fluids from the Kolsva pegmatite in Sweden and from the Tittling pegmatites in Bavaria. Remobilization of Be in late-magmatic, hydrothermal, and metamorphic regimes appears to be a reasonably common

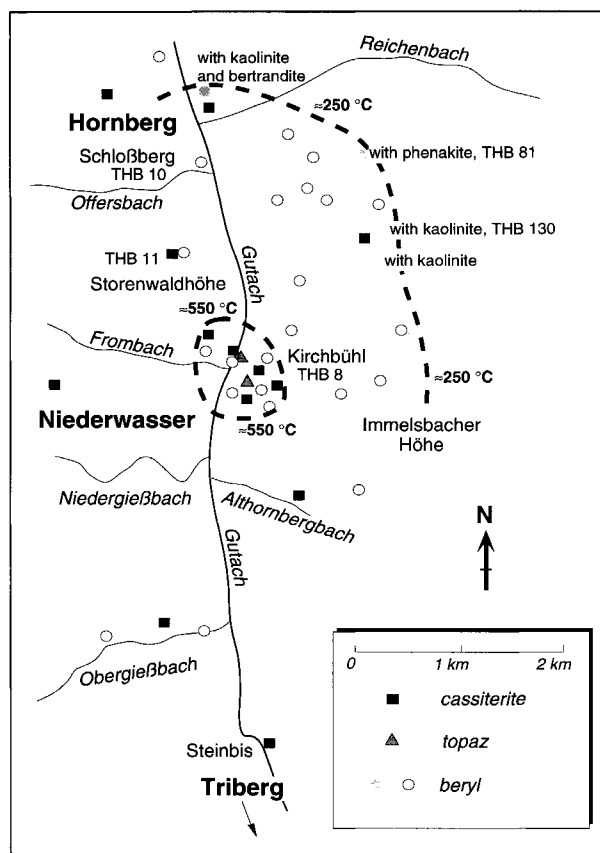


FIGURE 2. Enlargement of inset (study area) in Figure 1, showing the occurrences of beryl, topaz, and cassiterite in the area around Hornberg in the Triberg granite complex. The entire area consists of leucogranite.

phenomenon. Surprisingly, little information exists about transport mechanisms and the nature of Be^{2+} complexes. Černý (1968) mentioned fluoroberyllates as possibly important complexes in greisen and pegmatitic environments, but he also considered the Be^{2+} ion as important at low pH. Mobilization and transport of Be^{2+} , and especially formation of beryl in metamorphic environments, have been intensively studied in recent years, but very little work has been conducted on these same problems in the late-magmatic phase of granites. In this paper we describe the evolution of hydrothermal fluids and their effects on beryl stability within a cooling granite unit.

MINERALS AND MINERAL TEXTURES

Mineral textures in representative samples from the Triberg granite complex (Fig. 3) are described below and listed in Table 1. The sample localities are shown in Figure 2. These samples are typical examples of features seen throughout the study area. The beryllium minerals were identified by XRD analyses, and microprobe analyses were performed on feldspars and micas (see Markl and Schumacher 1996).

Sample THB 11 (locality shown in Fig. 2) shows grei-

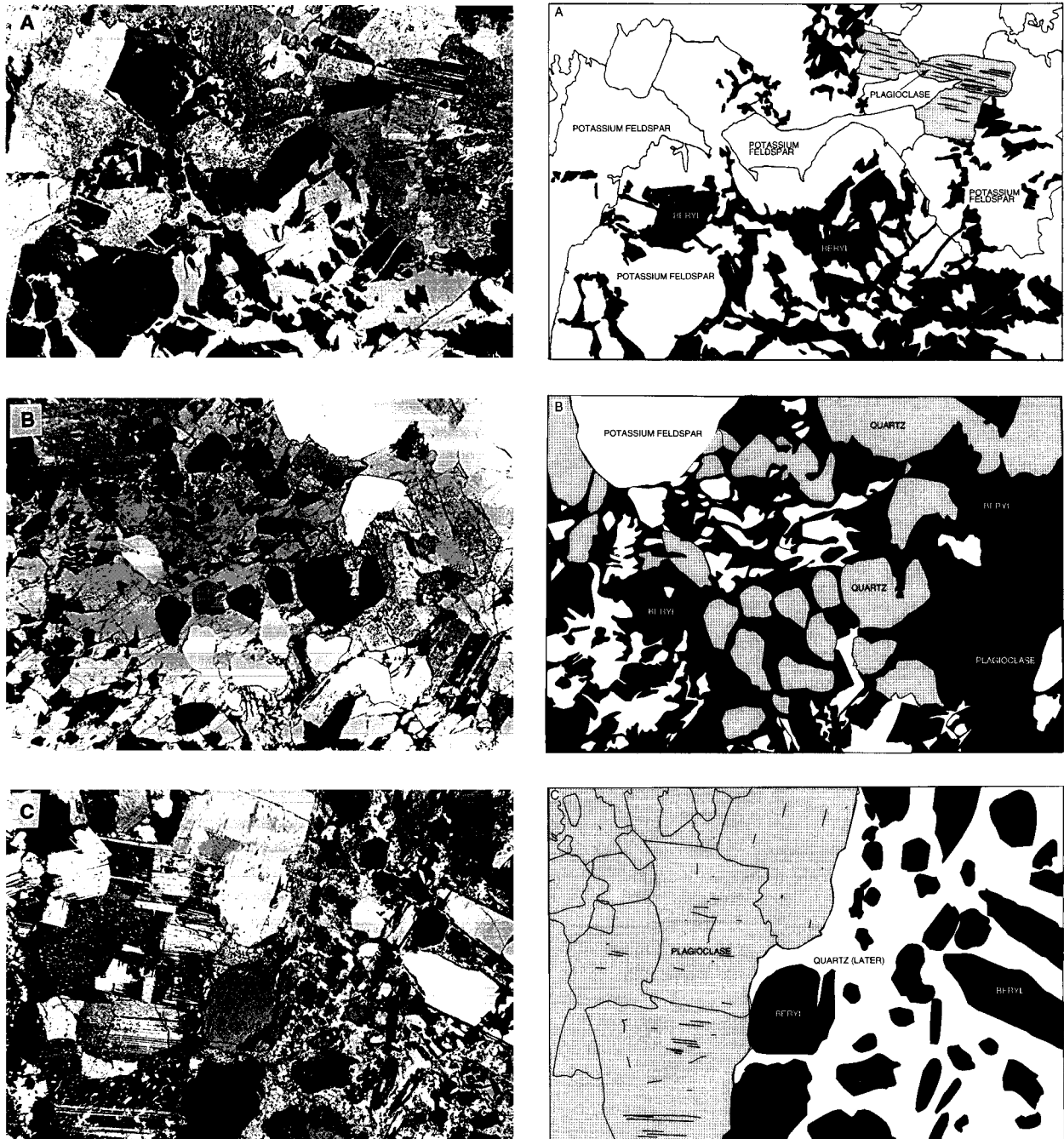


FIGURE 3. Photomicrographs (left) and micrographs (right) of beryl-bearing assemblages discussed in the text. (A) Beryl replacing potassium feldspar; (B) beryl replacing potassium feldspar in intergrowth with magmatically rounded quartz grains; (C) beryl crystals in a vug (right side of photograph) rimmed by albitized leucogranite (left side).

sen veins with reaction zones that reach up to 1 cm in leucogranitic host rock. The greisenization is most intense adjacent to the central fracture, and intensity decreases symmetrically outward. In the wall rock, plagioclase and potassium feldspar have been altered, although albite in the marginal sections has been altered less than potassium feldspar. In addition, the extent of silicification and de-

velopment of cassiterite and large white mica aggregates that are characteristic of the greisens decrease away from the central fracture.

Formation of secondary beryl

In sample THB 10 (Figs. 2 and 3), macroscopically pale blue beryl aggregates are extensively intergrown

TABLE 1. Primary and alteration assemblages with beryllium minerals from the Triberg granite complex, Germany

	Primary pegmatites	Secondary assemblages (probably one event, alteration temperatures decreasing from 1 to 6)						
		1	2	3a*	3b*	4	5	6
Beryl	X	X	X	X		C	C	C
Potassium feldspar	X		C		C			
Quartz	X	X	X	X	X	X	X	X
Plagioclase	O	X	X			O		
Muscovite	O	X			X			X
Fluorite		O						X
Cassiterite		O				X		
Phenakite					X			
Bertrandite							X	
Kaolinite						X	O	

Note: X = always present, O = sometimes present, C = corroded.

* Assemblages 3a and 3b occur in different parts of the same sample.

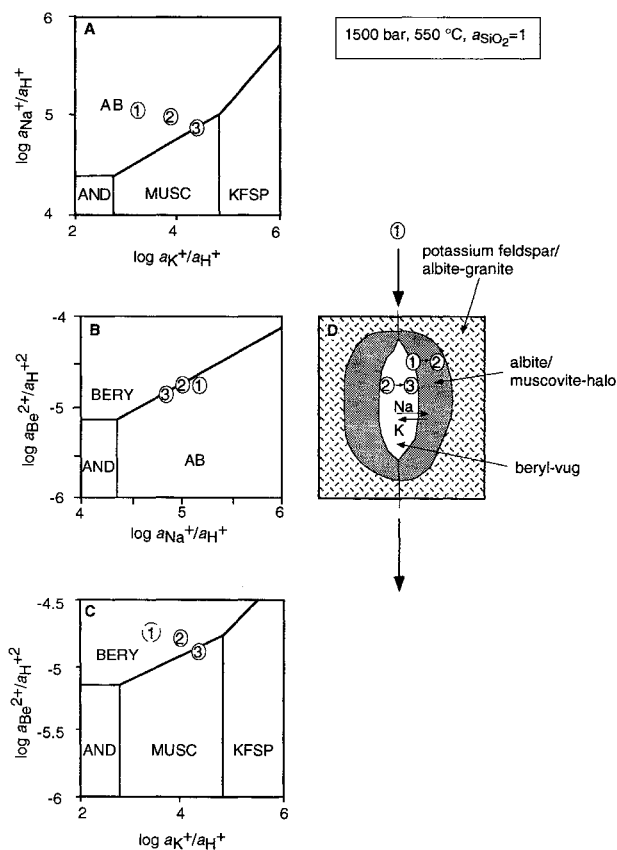


FIGURE 4. Explanation of secondary beryl formation. (A) Activity-activity diagram that shows replacement of potassium feldspar (KFSP) by albite (AB) and muscovite (MUSC) in the surrounding granite. (B) Activity-activity diagram that shows the attainment of beryl (BERY) saturation through the precipitation of albite. (C) Activity-activity diagram that shows muscovite forms at the end of the alteration process. (D) Schematic diagram of the beryl-bearing vugs and their alteration halo. The numbers enclosed in circles in A-C schematically show a possible correlation of the evolution of the fluid composition with the temporal and spatial evolution of the vug in D. AND = andalusite.

with the fine-grained leucogranite. In contrast to the pegmatitic beryl, these beryl grains are anhedral and about the same size (3–5 mm) as grains of the minerals of the host leucogranite. The beryl occurrence defines an ellipsoidal area of rock that extends a few centimeters. Although no visible fractures or veins are evident, the biotite in the beryl patch and in a zone that is several centimeters wide in the surrounding granite is strongly altered to chlorite and hematite. Hematite also commonly occurs in the beryl-bearing area, but it is not macroscopically visible in rock lacking beryl.

Figure 3 shows photomicrographs of the replacement textures of sample THB 10. The beryl is intergrown with and clearly replaces feldspar. The replacement by beryl appears to originate from fractures and grain boundaries inward. Figure 3b shows rounded quartz grains from the primary leucogranitic mineral assemblage completely surrounded by beryl and minor relics of potassium feldspar. These textures suggest the reaction of the magmatic potassium feldspar with a Be-bearing fluid. The quartz grains appear to retain their magmatic texture, and the albitic plagioclase from the granite that is in mutual contact with potassium feldspar and beryl was unaffected by the replacement of the neighboring potassium feldspar (Figs. 3a and 3b).

In sample THB 8, beryl occurs as terminated crystals in a granitic vug. The grains are up to 4 cm in length and, in rare cases, are of gem quality (pale blue aquamarine). The vug is surrounded by a zone of approximately 10 cm in which the fine-grained leucogranite is replaced by an albite + cassiterite + fluorite + muscovite rock (Figs. 3c and 3d). The albite is fresh and shows the chess-board pattern that is typical of albite that has metasomatically replaced potassium feldspar (e.g., Tröger 1967). The beryl crystals in the vug only rarely are intergrown with albite and appear to have nucleated and grown within the vug rather than through replacement of a preexisting phase. About 50 cm from this vug, a pegmatite contains partially corroded primary beryl crystals. This sample appears to be very similar to beryl crystals described by Oppelt (1991).

Replacement of beryl

In sample THB 130, a pegmatite that is about 30 cm across and that originally contained potassium feldspar, tourmaline, quartz, and beryl was strongly altered by reaction with the greisen fluids. This resulted in the complete replacement of potassium feldspar by muscovite and nearly complete replacement of beryl by kaolinite with coeval precipitation of cassiterite. Another texturally similar occurrence contains bertrandite in addition to kaolinite that has replaced beryl.

At sample locality THB 81, 200 m from locality THB 130, a pegmatitic lens shows beryl that is completely enclosed in quartz and unaltered, but where it was in contact with potassium feldspar, it is completely replaced by phenakite and muscovite.

Other samples show partially corroded pegmatitic beryl crystals in contact with fluorite and gem-quality aquamarine in vugs that are filled with iron hydroxide at the margin of a large pegmatite lens.

In summary, the typical occurrences are as follows: (1) greisen assemblages that are composed of muscovite and quartz \pm cassiterite \pm fluorite \pm topaz; (2) fresh beryl that occurs in pegmatite lenses with potassium feldspar, quartz, and albite; (3) secondary beryl that has replaced potassium feldspar in leucogranite; (4) secondary beryl with albite, quartz, muscovite, and, less commonly, fluorite and cassiterite; and (5) pegmatite lenses that have interacted with greisen fluids and that show partial to complete destruction of beryl and formation of muscovite and quartz with or without kaolinite, fluorite, bertrandite, phenakite, or cassiterite.

GEOCHEMISTRY

On the basis of the descriptions above, there are at least two late-magmatic to hydrothermal stages that are recorded by the Be mineralization. The earliest phase is the crystallization of the beryl-bearing pegmatites, which probably record temperatures of 600–650 °C, the approximate temperature of minimum melts in F- or B-bearing granitic systems (e.g., Burnham and Nekvasil 1986).

Crosscutting veins indicate that greisen formation was the next, but distinctly later, mineralization event. This second phase of hydrothermal activity occurred over a range of temperatures and in different chemical settings (bulk compositions). These hydrothermal events are probably related; it is nearly impossible to subdivide further the hydrothermal activity into distinct phases. The greisen fluids infiltrated along fractures and, in places, penetrated vug-rich granite. Normally, however, the greisen fluids affected only a few millimeters or centimeters of host rock adjacent to the central fracture. These fluids corroded the primary beryl crystals in places where the fractures intersected pegmatitic lenses. It is noteworthy that the temperature of the fluids is relatively unimportant in this case. Dissolution of beryl occurred over a range of temperatures (250–550 °C; Markl and Schumacher 1996). Consequently, the interaction of fluids with beryl record-

ed the late-magmatic through hydrothermal stage of the cooling history of the pluton. Kaolinite-bearing assemblages indicate temperatures below 300 °C (Hemley et al. 1980). At higher temperatures the beryl was partly leached and did not form an assemblage that bracketed the temperature of formation. These fluids were enriched in Be by dissolution of primary beryl over a wide range of temperatures.

The fluid-inclusion data that are reported in Markl and Schumacher (1996) indicate that the fluids are nearly pure H₂O with only 4% NaCl equivalent and without CO₂. The quantitative treatment of Be- and alkali-bearing fluids at 250 and 550 °C is shown in Figures 4–6. The diagrams were constructed using the program SUPCRT92 (Johnson et al. 1992) and its internally consistent database. This database includes all aqueous and solid species needed for our calculations with the exception of beryl and bertrandite. For these phases, data from Hemingway et al. (1986) and Barton (1986) were fitted to the thermodynamic functions used by SUPCRT92, and then these data were added to the database. It was also considered that SUPCRT92 and Barton (1986) use different Gibbs energies of formation for Al₂O₃. This problem was overcome by using consistent U.S. Geological Survey data. The addition of these phases effectively removed the constraint of internal consistency of the SUPCRT92 data. To test the validity of the augmented database, various equilibria involving beryl and bertrandite were calculated and compared with their experimentally located positions (Barton 1986). The results were essentially indistinguishable. There are two aqueous Be species in the SUPCRT92 database, Be²⁺ and BeO₂²⁻; we performed our calculations with Be²⁺ because it is more likely that this species is important in acid greisen-forming fluids.

The reactions that explain the interaction of the fluids with variable compositions and the various solid phases are shown on pH-normalized activity-activity diagrams (Figs. 4–6). This type of diagram was chosen because it was possible to show the chemical evolution of the fluids as the reactions proceeded.

High-temperature beryl precipitation

At some localities in vugs that were affected by hydrothermal fluids, nonpegmatitic beryl formed subhedral to euhedral crystals while the surrounding host granite was strongly altered to albite, muscovite, fluorite, and cassiterite. Potassium feldspar was completely consumed. Fluid-inclusion measurements and phase relations (Markl and Schumacher 1996) indicate fluid temperatures of about 550 °C.

A possible explanation of this alteration sequence is given in Figure 4. An initial fluid that was relatively rich in Be²⁺ and Na⁺ must have encountered the vug and may have mixed with, or completely replaced, the local fluid. The resulting composition was a fluid such as fluid 1 in Figure 4. This initial fluid began to react with the granite, causing albitization of potassium feldspar by K-Na exchange (Fig. 4A). As albitization proceeded, the Na con-

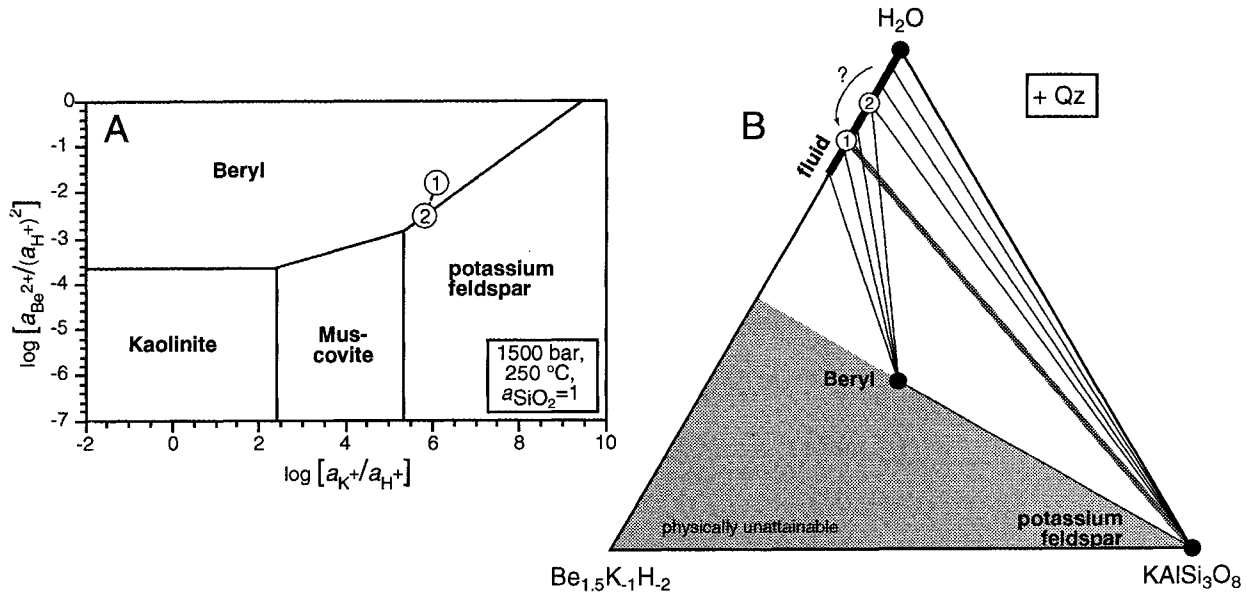


FIGURE 5. Explanation of secondary beryl replacing potassium feldspar. (A) Activity-activity diagram that shows the influx of a Be-enriched fluid and the subsequent evolution. (B) Composition diagram that shows the possible gradient set up between potassium feldspar and the introduced fluid (wide gray line). The variation in fluid composition assumes that the fluid is capable of compositional variation along the $\text{Be}_{1.5}\text{K}_{-1}\text{H}_{-2}$ exchange vector.

tent of the fluid decreased and became saturated with beryl (fluid 2; Figs. 4B and 4C). The potassium feldspar then became unstable with respect to both beryl and albite (fluid 2; Figs. 4A and 4C). Beryl and albite continued to form at the expense of potassium feldspar, which buffered the fluid as it changed composition toward the muscovite-stability field (fluid 3; Fig. 4A–4C). Upon reaching composition 3 (Fig. 4), muscovite became the third and final phase to form at the expense of potassium feldspar. At this point, all the potassium feldspar in the area around the vug that was affected by the fluid was consumed and the reactions ceased.

Figure 4 explains the observed alterations and the sequence of their development but does not deal with their growth locations. Beryl precipitated on the vug walls, whereas secondary albite from the alteration zone around the vug shows the chess-board pattern typical for potassium feldspar replacement. We suggest that this rapid exchange of K^+ in the rock with Na^+ in the fluid occurred primarily in the granite around the vug. Beryl precipitation, which must have also involved Al mobility, occurred at the walls of the vug and in contact with the largest volume of fluid (Fig. 4D).

Low-temperature beryl formation

Secondary beryl that replaced potassium feldspar (sample THB 10; Fig. 3) must have resulted from a fracture in the granite that acted as fluid conduit. However, at the reaction site no vug was present. Beryl directly replaced potassium feldspar. Interestingly, coexisting primary albitic plagioclase remains absolutely unaltered, which suggests that fluids were not only high in Be^{2+} but

also high in Na^+ , as was also suggested by sample THB 8 (Fig. 4). Temperatures were probably in the 250–300 °C range (Markl and Schumacher 1996).

The replacement of the potassium feldspar by beryl requires the influx of a fluid that is enriched in Be. As in the other examples, a fluid need not have been present initially, but significant amounts of fluid had to be present at the time of reaction. Influx of a fluid such as fluid 1 (Fig. 5A) would be out of equilibrium with potassium feldspar, which would immediately form beryl. The fluid would move toward composition 2 (Fig. 5). Figure 5B shows that the proportions of fluid to potassium feldspar (wide gray line in Fig. 5B) at the start of the reaction would determine the proportions of the solid phases at the end of the reaction. At extremely high ratios of fluid to potassium feldspar, potassium feldspar would be completely consumed (i.e., fluid-to-potassium feldspar ratios that lie within the two-phase field fluid-beryl; Fig. 5B). At lower ratios of fluid to potassium feldspar (within the three-phase field beryl-potassium feldspar-fluid), the fluid would reach composition 2, and the reaction would cease, leaving the potassium feldspar partially replaced by beryl.

Low-temperature beryl alteration

At several localities, beryl was altered at low temperature. This resulted either in the coeval replacement of beryl by kaolinite \pm minor bertrandite and of potassium feldspar by muscovite in the immediately enclosing granite, or in the reaction of beryl and potassium feldspar with fluid to form phenakite and quartz. On the basis of the observed kaolinite-bearing assemblages and the calculat-

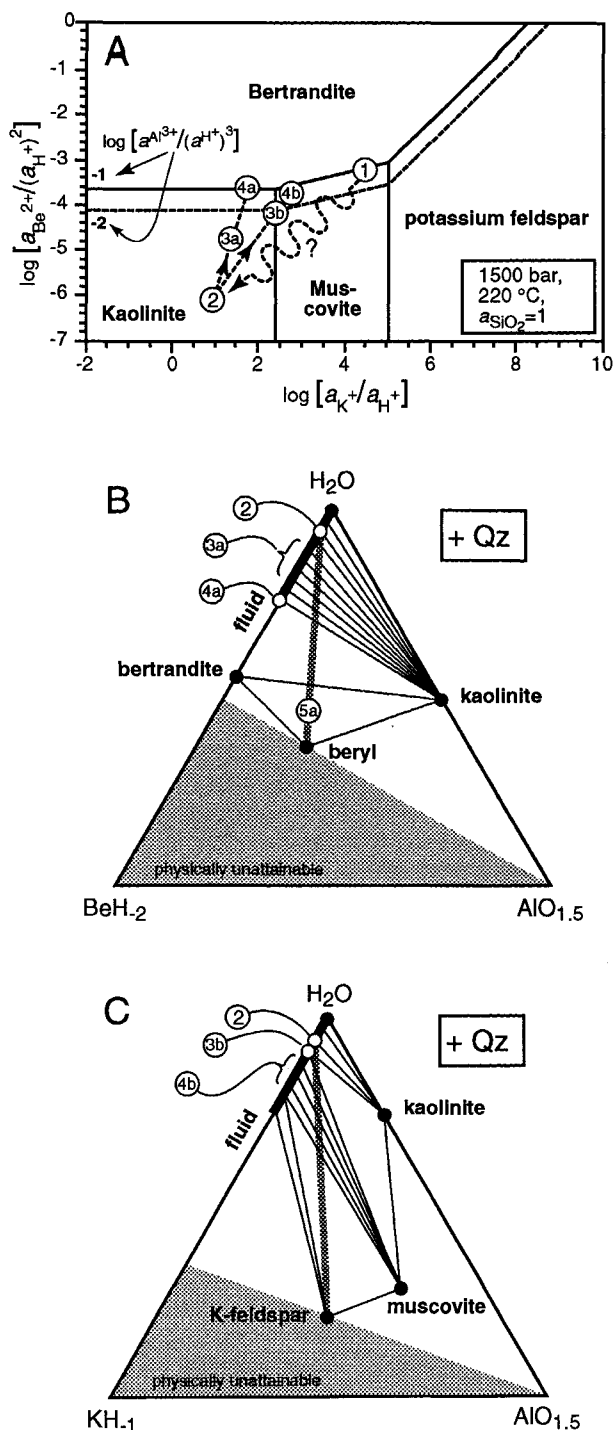


FIGURE 6. Explanation of secondary beryl replacement by kaolinite ± bertrandite. (A) Activity-activity diagram that shows the evolution of fluids controlled by the dissolution of beryl and potassium feldspar. The stability field of bertrandite depends on the Al content of the fluid and is therefore contoured for two values of $\log [a_{\text{Al}^{3+}}/(a_{\text{H}^+})^3]$. (B) Composition diagram that shows the possible gradient set up between beryl and the introduced fluid (wide gray line). The variation in fluid composition assumes that the fluid is capable of solution along the BeH₂ exchange vector. (C) Composition diagram that shows the possible gradient set up between potassium feldspar and the introduced fluid (wide gray line). The variation in fluid composition assumes that the fluid is capable of compositional variation along the KH₁ exchange vector. The circled numbers in the diagrams refer to the following model. (1) Possible composition of fluid coexisting with beryl + potassium feldspar at temperatures above bertrandite + kaolinite stability, if a fluid phase was present. (2) Influx of Be- and K-poor fluid: Either local fluid composition 1 is dramatically changed, or essentially fluid-free, beryl + potassium feldspar assemblages are exposed to fluid composition (2). Depending on the effective fluid-to-solid ratio, beryl is converted to kaolinite by (3a) beryl + 6H⁺ = kaolinite + 3Be²⁺ + 4 quartz + 2H₂O or to bertrandite + kaolinite in a Be²⁺-saturated fluid by (4a) kaolinite + bertrandite + 5 quartz. Potassium feldspar breaks down to kaolinite by (3b) 2Kfsp + 2H⁺ + 2H₂O = kaolinite + 2K⁺ + 4 quartz or to muscovite by (4b) 3Kfsp + 2H⁺ = muscovite + 2K⁺ + 6 quartz. (5a) Where the effective fluid-to-beryl ratio is very low, fluid is completely consumed, leaving relict beryl + bertrandite + kaolinite.

however, any new fluid could have mixed with, or replaced, a preexisting fluid that was stable with beryl. Nevertheless, the new fluid must have been abundant enough to have dominated the phase relations in rock with volumes up to 50 dm³.

This fluid, relatively low in Be²⁺ and K⁺, would have been out of equilibrium with both beryl and potassium feldspar. The presence of these chemical gradients (shown as wide gray lines in Figs. 6B and 6C) results in the incongruent dissolution of beryl and potassium feldspar. The extent of each reaction depends on the effective fluid-to-solid ratio up to the point the reaction ceased. At relatively high fluid-to-beryl ratios, beryl would be completely replaced by kaolinite and eventually bertrandite (fluid 4a; Figs. 6A and 6B). At effective fluid-to-beryl ratios less than those of fluid 4a (Figs. 6A and 6B), relict beryl + kaolinite ± bertrandite ± phenakite (dependent on the temperature of the replacement reaction and the extent of the evolution of the fluid) would be left.

Similarly, the fluid that caused the beryl alteration could be responsible for the replacement of the potassium feldspar by white mica (path 2 → 3b in Figs. 6A and 6C). Again, depending on the effective fluid-to-feldspar ratio (Fig. 6C), the potassium feldspar could be completely to partially replaced by muscovite (Figs. 6A and 6C). For even higher ratios of fluid to solid, muscovite could be replaced by kaolinite. These latter textures have not been demonstrated; all observations to date suggest that only

ed phase relations (Hemley et al. 1980; see also Markl and Schumacher 1996), this stage of beryl alteration is estimated to have occurred at about 220 °C (Fig. 6). A model for this stage of beryl alteration postulates the influx of a Be²⁺- and K⁺-poor fluid (kaolinite-stability field; Fig. 6A). Beryl was not stable with this fluid and reacted to form kaolinite. No fluid had to be present initially;

the white mica was generated by the break down of potassium feldspar. The formation of kaolinite is texturally related to the dissolution of the beryl. It is also important to note that, in contrast to high-temperature cases, the beryl and the potassium feldspar behave as two separate bulk compositions that are affected differently by similar fluids.

The presence of cassiterite in these low-temperature assemblages indicates that the fluids were related to the greisen-forming fluids and that the composition of this Be²⁺- and K⁺-poor fluid was externally controlled. At least locally, a Be²⁺-rich fluid evolved that reached concentrations high enough to stabilize new Be phases (phenakite and bertrandite). The reactions probably ceased when the supply of fluid was exhausted.

DISCUSSION AND CONCLUSIONS

Na-K-Be variations in the fluid

In the activity diagrams in Figure 4, the final fluid compositions are reasonably well constrained by the assemblages and fluid-inclusion data. The starting fluid compositions are more problematic; however, because textures indicate that precipitation of additional phases closely follows albite formation, it can be inferred that the starting fluids lie reasonably near the relevant field boundaries of albite. Consequently, the assumed composition of the initial fluid (Fig. 4) is probably a reasonable approximation of the actual fluids involved in the alteration process.

As shown above, the replacement of potassium feldspar by albite is a common feature of the alteration. The net effect is to decrease the Na content while increasing the K content of the fluid. The importance of this chemical variation to beryl formation is shown in Figure 4; in that example, the change in Na and K contents drove the fluid into the beryl-stability field without major changes in the Be content of the fluid.

Using both the fluid-inclusion measurements (Markl and Schumacher 1996) and the calculated phase relations (Fig. 4), it is possible to estimate the actual pH of the fluids that caused the alteration. The 4% NaCl from the fluid inclusions corresponds to 0.68 m/l. The value of $\log(a_{\text{Na}^+}/a_{\text{H}^+})$ of 5.1 (point 1 in Fig. 4A) was chosen on the basis of the assumption that none of the fluid compositions was far removed from the various stable assemblages. If these data are combined, the pH is estimated to be about 5.3.

Estimates of the changes in relative concentrations of K, Na, and Be in the fluid as the reactions proceed can also be obtained from Figure 4. For this reaction sequence, the ratios of Na/K and Be/K should both decrease more than one order of magnitude (Na/K from about 80 to 3, Be/K from about $1.3 \times 10^{-8} \times a_{\text{H}^+}$ to $6.3 \times 10^{-10} \times a_{\text{H}^+}$), whereas Be/Na increases very slightly (from about $1.6 \times 10^{-10} \times a_{\text{H}^+}$ to $2 \times 10^{-10} \times a_{\text{H}^+}$, all values estimated from Fig. 4). This increase in Be/Na seems surprising because of the formation of beryl, but it results from the extensive simultaneous formation of albite.

Estimations of the absolute element ratios are more difficult, but, if the values and the calculated stability fields in Figure 4 are used, then Na/K should change from about 80 to 3, which agrees well with the fluid-inclusion measurements. These show about 4% NaCl equivalent with minor CaCl₂ but no KCl. Interestingly, Be/Na and Be/K ratios are very low, although beryl precipitates.

Origin of the fluids

On the basis of these observations, the fluids that are responsible for all the reactions are basically greisen fluids, which is indicated by the common occurrence of cassiterite and fluorite in the alteration zones. These greisen fluids interacted with a variety of local assemblages over a range of temperatures. The exact nature of the observed alteration depends on which combination of all these factors was operating at each locality. In some areas, there is evidence for both the enrichment and depletion of Be in the fluid. For example, where beryl replaces potassium feldspar (Fig. 5), a Be-enriched fluid is necessary. The source of the Be²⁺-enriched fluids is problematic, but the presence of strongly altered pegmatite beryl in the vicinity of the secondary beryl indicates that dissolution of primary beryl is the source. Consequently, no additional Be²⁺-enriched magmatic or hydrothermal fluid from an outside source is required. A sample with fluorite filling the cavities in partly dissolved pegmatitic beryl suggests that these fluids were the same fluids that formed the cassiterite-bearing greisen assemblages in this area [see Markl and Schumacher (1996) for detailed description]. And this in turn fits very well with the observation of fluorite and cassiterite in the samples of secondary beryl described above.

The fluids that are responsible for this alteration could have come from various sources. Here they are greisen-related fluids, but any reactive hydrothermal fluid could produce a similar style of alteration.

Gem-quality beryl: The role of the local environment

There are two types of occurrences of secondary beryl. Secondary gem-quality beryl is restricted to vugs, where fluids were able to collect. Where beryl formed, but no free space was available, replacement textures after potassium feldspar developed. Around the vugs, relatively wide (20 cm zones) alteration halos formed; in contrast, the fractures away from the vugs show only very narrow (1 cm) alteration halos. This suggests that, after the fluids were emplaced in the fractures and vugs, the amount of subsequent alteration depended on the amount of reactive fluid available and the duration of the interaction. The width of the interaction zones probably depended on the permeability of the adjacent rock. On the basis of the width of the alteration zones, the granite enclosing the vugs must have had higher permeability than is generally seen around the narrow linear fractures. These observations seem to suggest that most of the interactions that most strongly influenced the chemistry of the fluids occurred in the vicinity of the vugs. This is consistent with

the observation that most of the secondary minerals, including gem-quality beryl, grew in the vicinity of the vugs.

Model of Be redistribution

Textures suggest that replacement of various minerals occurred during the rapid influx of fluid that was out of chemical equilibrium with the local mineral assemblage. As summarized above (see also Markl and Schumacher 1996), these fluids display a range of compositions and were active over a range of temperatures. We envision a scenario in which fractures, possibly due to thermal contraction, were propagating. Over time and at various temperatures, hydrothermal fluids encountered these fractures and moved rapidly to new locations in the leucogranite. Locally, these fluids reacted extensively with the surroundings, and, depending on rock and fluid compositions, effective fluid-to-rock ratio, temperature, and pressure, the replacement textures that were outlined above were produced.

The above observations seem to indicate that the Be mineralization of this granite unit records numerous steps in the cooling history and accompanying chemical evolution of the late-magmatic to hydrothermal fluids. In the case investigated here, the fluids that caused the mineralization appear to have had a local source. However, many hydrothermal fluids could initiate a similar series of mineralizing reactions upon encountering Be-enriched granitic rocks.

ACKNOWLEDGMENTS

We are very grateful to F. Pfundstein (at Konstanz), H. Stempel (at Hornberg), and D. Schrenk (at Fischerbach) for supplying some of the important samples that were used in this study. We also thank K. Fesenmeier, who prepared the thin sections, and H. Schlegel, who performed XRD analyses on several samples. We thank D. Burt and M. Barton for extremely helpful and constructive reviews.

REFERENCES CITED

- Barton, M.D. (1986) Phase equilibria and thermodynamic properties of minerals in the BeO-Al₂O₃-SiO₂-H₂O (BASH) system, with petrological applications. *American Mineralogist*, 71, 277–300.
- Burnham, C.W., and Nekvasil, H. (1986) Equilibrium properties of granite pegmatite magmas. *American Mineralogist*, 71, 239–263.
- Burt, D.M. (1975) Beryllium mineral stabilities in the model system CaO-BeO-SiO₂-P₂O₅-F₂O₋₁, and the breakdown of beryl. *Economic Geology*, 70, 1279–1292.
- Cerny, P. (1968) Berylliumwandlungen in Pegmatiten: Verlauf und Produkte. *Neues Jahrbuch für Mineralogie Abhandlungen*, 108, 166–180.
- Franz, G., and Morteani, G. (1984) The formation of chrysoberyl in metamorphosed pegmatites. *Journal of Petrology*, 25, 27–52.
- Hemingway, B.S., Barton, M.D., Robie, R.A., and Haselton, H.T. (1986) Heat capacities and thermodynamic functions for beryl, Be₃Al₂Si₆O₁₈, phenakite, Be₂SiO₄, euclase, BeAlSiO₄(OH), bertrandite, Be₂Si₂O₇(OH)₂, and chrysoberyl, BeAl₂O₃. *American Mineralogist*, 71, 557–568.
- Hemley, J.J., Montoya, J.W., Marinenko, J.W., and Luce, R.W. (1980) Equilibria in the system Al₂O₃-SiO₂-H₂O and some general implications for alteration/mineralization processes. *Economic Geology*, 75, 210–228.
- Jahns, R.H., and Burnham, C.W. (1969) Experimental studies of pegmatite genesis: I. A model for the derivation and crystallization of granitic pegmatites. *Economic Geology*, 64, 843–864.
- Johnson, J.W., Oelkers, E.H., and Helgeson, H.C. (1992) SUPCRT92: A software package for calculating the standard molal thermodynamic properties of minerals, gases, aqueous species, and reactions from 1 to 5000 bars and 0 to 1000 °C. *Computers and Geosciences*, 18, 899–947.
- Markl, G. (1994) Chemische und thermische Gradienten spätmagmatischer Fluide bei der Bildung von Cassiterit-führenden Greisen: Beobachtungen an Mineralassoziationen im Triberger Granit-Komplex südlich von Hornberg, Schwarzwald, SW-Deutschland, 137 p. M.S. thesis, Institute of Mineralogy, Petrology and Geochemistry, Freiburg, Germany.
- Markl, G., and Schumacher, J.C. (1996) Cassiterite-bearing greisens and late-magmatic mineralization in the Variscan Triberg Granite Complex, Schwarzwald, Germany. *Economic Geology*, in press.
- Mårtensson, C. (1960) Euklas und Bertrandit aus dem Feldspatpegmatit von Kolsva in Schweden. *Neues Jahrbuch für Mineralogie Abhandlungen*, 94, 1248–1252.
- Oppelt, W. (1991) Neue Beryllfunde aus dem Gebiet von Niederwasser. *Der Erzgräber*, 5, 3–6.
- Schleicher, H. (1978) Petrologie der granitporphyre des Schwarzwaldes. *Neues Jahrbuch für Mineralogie Abhandlungen*, 132, 153–181.
- (1984) Der Triberger Granit. *Fortschritte der Mineralogie*, 62, 91–98.
- (1994) Collision-type granitic melts in the context of thrust tectonics and uplift history (Triberg granite complex, Schwarzwald, Germany). *Neues Jahrbuch für Mineralogie*, 166, 211–237.
- Schleicher, H., and Fritsche, R. (1978) Zur Petrologie des Triberger Granites (Mittlerer Schwarzwald). *Jahreshefte des geologischen Landesamtes Baden-Württemberg*, 20, 15–41.
- Tennyson, C. (1960) Berylliumminerale und ihre pegmatitische Paragenese in den Graniten von Tittling/Bayrischer Wald. *Neues Jahrbuch für Mineralogie Abhandlungen*, 94, 1253–1265.
- Tröger, W.E. (1967) Optische Bestimmung der gesteinsbildenden Minerale, Teil 2, Textband. Schweizerbarth, Stuttgart.
- Werchau, A., Schleicher, H., and Kramm, U. (1989) Erste Altersbestimmungen an Monaziten des Schwarzwaldes. *European Journal of Mineralogy*, 1, 198.

MANUSCRIPT RECEIVED SEPTEMBER 14, 1995

MANUSCRIPT ACCEPTED SEPTEMBER 17, 1996